

Activation of human medial prefrontal cortex during autonomic responses to hypoglycemia

Denise Teves*, Tom O. Videen†, Philip E. Cryer*, and William J. Powers†*

*Division of Endocrinology, Metabolism, and Lipid Research of the Department of Internal Medicine, Washington University School of Medicine, Campus Box 8127, 660 South Euclid Avenue, St. Louis, MO 63110; and †Departments of Neurology and Radiology, Washington University School of Medicine, East Building Imaging Center, Campus Box 8225, 4525 Scott Avenue, St. Louis, MO 63110

Edited by Marcus E. Raichle, Washington University School of Medicine, St. Louis, MO, and approved February 5, 2004 (received for review October 30, 2003)

Studies in humans implicate the medial prefrontal cortex (MPFC) in complex cognitive and emotional states. We measured regional cerebral blood flow (CBF) four times each during euglycemia (5.2 ± 0.2 mmol/liter) and hypoglycemia (3.0 ± 0.3 mmol/liter) in nine normal human volunteers. Autonomic responses during hypoglycemia were manifested by increases in neurogenic symptoms, heart rate, and plasma levels of epinephrine, norepinephrine, and pancreatic polypeptide. Typical symptoms of hypoglycemia were mild, and none reflected evidence of cognitive or emotional stress. Quantitative CBF fell 6–8% in the cerebrum, brainstem, and cerebellum. Analysis of regional CBF differences identified neuronal activation during hypoglycemia in bilateral MPFC (areas 24 and 32) and bilateral thalamus. These results provide evidence that the MPFC participates in the autonomic responses to simple physiological stimuli in humans.

Most studies of the medial prefrontal cortex (MPFC) in human subjects have focused on its role in complex cognitive and emotional states (1–8). In particular, portions of the anterior cingulate cortex (ACC) are thought to play an important role in emotional processing (1, 2). Anatomic connections between the MPFC and autonomic structures in the brainstem and hypothalamus are well recognized (9, 10). Previous human studies relating the MPFC and autonomic states have concentrated on the interplay of autonomic arousal and emotional, cognitive, or volitional behaviors (3–5, 11, 12). Studies of brain participation in autonomic responses to more basic physiological stimuli such as hypoglycemia have implicated subcortical structures (12–14). There has been little study of cortical involvement in basic autonomic responses (15).

We used positron emission tomography (PET) to compare regional neuronal activity in nine normal subjects during normoglycemia and hypoglycemia. Typical physiological and biochemical evidence of activation of the autonomic nervous system was demonstrated in the absence of cognitive or emotional stress. During hypoglycemic autonomic activation, areas of increased neuronal activity were observed in bilateral MPFC (areas 24 and 32) and bilateral thalamus. These results provide evidence that the MPFC participates in the autonomic responses to simple physiological stimuli in humans.

Methods

Subjects. Nine healthy subjects (five women and four men) gave their informed consent to participate in this study. Their mean age was 24 years (range: 18–32 years). Their mean body mass index was 23.3 kg/m^2 (range: 19 to 32 kg/m^2). This research was conducted at the Washington University General Clinical Research Center and the Neurology-Neurosurgery Intensive Care Unit PET Research Facility. All aspects were approved by the Human Studies Committee and the Radioactive Drug Research Committee of Washington University in accord with the Declaration of Helsinki.

Experimental Design. The subjects reported to the Washington University General Clinical Research Center after an overnight

fast. Two i.v. lines (one for infusion of insulin and glucose and one for injection of [^{15}O]water) were inserted into antecubital veins, and a radial artery was cannulated for blood sampling. Subjects remained supine throughout. Insulin ($2.0 \text{ milliunits}\cdot\text{kg}^{-1}\cdot\text{min}^{-1}$) was infused from 0 through 180 min, arterial plasma glucose concentrations were measured every 5 min, and 20% glucose was infused in variable doses to clamp plasma glucose concentrations at ≈ 5.0 mmol/liter (90 mg/dl) from 0 through 90 min and then at ≈ 3.0 mmol/liter (54 mg/dl) through 180 min. Regional cerebral blood flow (rCBF) was determined with PET four times during euglycemia and four times during hypoglycemia (see below). In addition to the PET sampling, arterial blood samples for the analytes listed below were drawn, and heart rates and blood pressures (Propaq Encore, Protocol Systems, Beaverton, OR) were recorded at –15, 0, 30, 60, 90, 120, 150, and 180 min. The electrocardiogram was monitored throughout. Symptoms of hypoglycemia also were quantitated at –15, 0, 30, 60, 90, 120, 150, and 180 min by asking the subjects to score from 0 (none) to 6 (severe) each of 12 symptoms: six neurogenic (autonomic) symptoms (adrenergic: heart pounding, shaky/tremulous, and nervous/anxious; cholinergic: sweaty, hungry, and tingling) and six neuroglycopenic symptoms (difficulty thinking/confused, tired/drowsy, weak, warm, faint, and dizzy) (16).

Analytical Methods. Plasma glucose concentrations were measured with a glucose oxidase method (YSI Glucose Analyzer 2, Yellow Springs Instruments). Plasma epinephrine and norepinephrine were measured with a single isotope derivative (radioenzymatic) method (17). Plasma insulin, C-peptide, glucagon, pancreatic polypeptide, cortisol, and growth hormone were measured with radioimmunoassays (18–22).

PET and Magnetic Resonance Imaging. PET studies were performed with a Siemens/CTI (Knoxville, TN) ECAT EXACT HR 47 tomograph located in the Neurology-Neurosurgery Intensive Care Unit PET Research Facility (23). Subjects were positioned in the tomograph such that the entire brainstem was included within the 15-cm axial field of view. As a result, the vertex of the brain was not included within the study area. An individual transmission scan was obtained for each patient and used for subsequent attenuation correction of emission scan data. rCBF was measured with a 40-sec emission scan after bolus i.v. injection of 50 mCi of [^{15}O]water (1 Ci = 37 GBq) using an adaptation of the Kety autoradiographic method (24–26). PET scans were acquired in the two-dimensional mode (interslice septa extended). Radioactivity in arterial blood was measured simultaneously with an automated blood sampler. The arterial

This paper was submitted directly (Track II) to the PNAS office.

Abbreviations: MPFC, medial prefrontal cortex; ACC, anterior cingulate cortex; PET, positron emission tomography; CBF, cerebral blood flow; rCBF, regional CBF; MR, magnetic resonance.

†To whom correspondence should be addressed. E-mail: wjp@npg.wustl.edu.

© 2004 by The National Academy of Sciences of the USA

Table 1. Physiological and endocrine responses to hypoglycemia (mean ± SD)

	Normoglycemia	Hypoglycemia	<i>P</i> *
Plasma glucose, mmol/liter	5.2 ± 0.2	3.0 ± 0.3	—
Heart rate, beats per min	62 ± 9	71 ± 10	0.004
Systolic blood pressure, mmHg (1 mmHg = 133 P)	126 ± 14	128 ± 17	0.77
Diastolic blood pressure, mmHg	55 ± 10	51 ± 9	0.20
Arterial pCO ₂ , mmHg	37.5 ± 3.0	37.6 ± 2.7	0.92
Epinephrine, pmol/liter	210 ± 150	4340 ± 2010	0.0002
Norepinephrine, nmol/liter	1.45 ± 0.37	2.03 ± 0.56	0.007
Pancreatic polypeptide, pmol/liter	12 ± 6	57 ± 28	0.001
Glucagon, pmol/liter	26 ± 4	38 ± 11	0.006
Cortisol, nmol/liter	290 ± 70	460 ± 80	0.0002
Growth hormone, pmol/liter	35 ± 17	630 ± 290	0.0006

**P* values by paired *t* test of mean values during normoglycemia (30–90 min) and hypoglycemia (120–180 min).

time/radioactivity curve recorded by the sampler was corrected for delay and dispersion by using previously determined parameters. One to four arterial blood samples for analysis of pCO₂ were collected during normoglycemia and during hypoglycemia (Instrumentation Laboratory, Lexington, MA). PET images were reconstructed by using filtered back-projection and measured attenuation and then smoothed with a three-dimensional Gaussian filter to a resolution of 10 mm full-width at half-maximum. Data from the arterial time/radioactivity curve was used to generate images of quantitative rCBF (25, 26).

Each subject also underwent structural magnetic resonance (MR) imaging of the brain with a 1.5-T system (Magnetom Sonata, Siemens, Erlangen, Germany). A three-dimensional magnetization-prepared rapid gradient echo sequence (1900/1100/3.93 repetition time/inversion time/echo time; flip angle = 15°) was acquired in a sagittally oriented slab (160 mm thick, 128 partitions, 256 mm field of view) and reconstructed into a 256 × 256 matrix (1 × 1 × 1.25-mm pixels).

Each subject's eight PET images and single MR image were co-registered to each other (27, 28). Using the MR image as a template, the brain was divided into cerebellum, brainstem, and

hemispheres. For each subject, quantitative rCBF values during normoglycemia and hypoglycemia for each of these three structures was calculated as the mean of the four rCBF studies performed during each state.

Statistical Methods. The values obtained at the 30-, 60-, and 90-min time points during normoglycemia and the 90-, 120-, and 180-min time points during hypoglycemia were averaged for each subject's symptom scores and physiological, blood biochemical, and quantitative CBF measurements. Comparisons between values during normoglycemia and hypoglycemia were performed with paired *t* tests. Raw *P* values are presented; they are not corrected for increased alpha error because of multiple comparisons.

For analysis of relative rCBF changes, all individual images were normalized by using mean whole-brain counts and co-registered to a standard mean blood flow image in Talairach atlas space (27–29). For each subject, the mean of the four studies performed during each state was used for statistical analysis. All voxels within sampled brain were examined with SPM99 (www.fil.ion.ucl.ac.uk/spm) by using a random-effects model with multiple-comparisons correction for the entire volume. *T* values were computed at each voxel, and clusters of at least 90 voxels (1 resel) with uncorrected *P* < 0.005 were identified (*t* ≥ 3.36, *df* = 8). The statistical significance of these clusters was computed and corrected for the number of possible clusters of their size and magnitude within the brain volume (30, 31).

Results

Clear evidence of sympathoadrenal (neurogenic symptoms, heart rate, epinephrine, and norepinephrine), parasympathetic (pancreatic polypeptide), and hypothalamic-pituitary (cortisol and growth hormone) responses to hypoglycemia was demonstrated (16) (Table 1 and Fig. 1). Typical neurogenic and neuroglycopenic symptoms were reported by the subjects (16) (Fig. 1). All these symptoms were mild, and none reflected evidence of cognitive or emotional stress. It is notable that

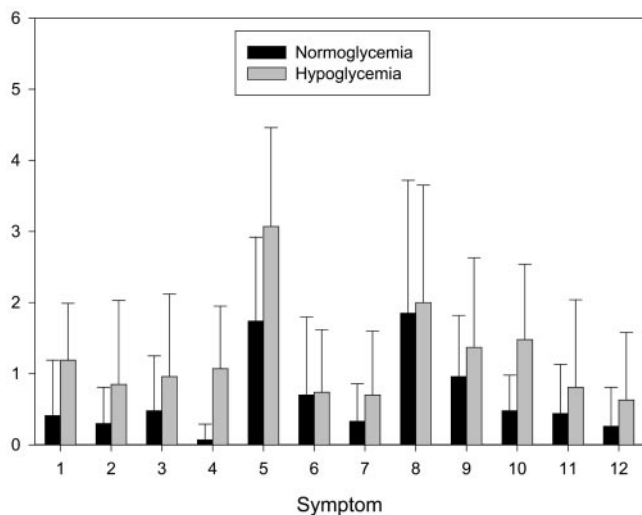


Fig. 1. Symptoms reported during normoglycemia and hypoglycemia. Every 30 min, subjects were asked to score the following symptoms on a linear scale from 0 (none) to 6 (severe): 1, heart pounding (*P* = 0.002); 2, shaky/tremulous (*P* = 0.042); 3, nervous/anxious (*P* = 0.076); 4, sweaty (*P* = 0.005); 5, hungry (*P* = 0.007); 6, tingling (*P* = 0.889); 7, difficulty thinking (*P* = 0.051); 8, tired/drowsy (*P* = 0.616); 9, weak (*P* = 0.047); 10, warm (*P* = 0.011); 11, faint (*P* = 0.084); and 12, dizzy (*P* = 0.030).

Table 2. Quantitative cerebral blood flow responses to hypoglycemia [ml·100 g⁻¹·min⁻¹ (mean ± SD)]

	Baseline	Hypoglycemia	% Change	<i>P</i> *
Cerebral hemispheres	56 ± 14	52 ± 14	-7.8 ± 5.4	0.003
Brainstem	55 ± 13	52 ± 13	-6.4 ± 4.7	0.005
Cerebellum	62 ± 18	58 ± 18	-8.0 ± 4.2	0.007

**P* values by paired *t* test of mean values during normoglycemia and hypoglycemia.

Table 3. Statistically significant clusters of voxels with relatively increased or decreased activity during hypoglycemia

	Voxels	T	P	X	Y	Z
Increased activity						
Left thalamus	957	14.72	0.001	-11	-23	6
Right thalamus		8.32		6	-23	8
Right ventral globus pallidus	150	10.19	0.010	10	-1	-5
Left MPFC	908	9.71	0.001	-7	27	17
Right MPFC		8.76		6	33	15
Right temporal cortex	173	9.30	0.004	40	4	16
Right orbital prefrontal cortex	485	8.66	0.001	26	38	0
Right sensorimotor cortex	235	7.74	0.001	38	-28	24
Periaqueductal grey	11	3.86	NS	-2	-39	-16
Decreased activity						
Right hippocampus	146	8.81	0.012	20	-40	9
Right temporal cortex	132	8.31	0.020	44	-12	-13

Statistically significant clusters of voxels with increased or decreased activity ($t \geq 3.36$) relative to whole-brain activity during hypoglycemia. Voxels = number of suprathreshold voxels per cluster ($8 \text{ mm}^3/\text{voxel}$); T = peak t value for a single voxel within each cluster; P = corrected cluster-level probability. Clusters for the thalamus and MPFC merged across the midline. Center-of-volume stereotactic coordinates (X - Z) are positive for right, anterior, and superior, respectively.

among these symptoms is the lack of a significant change in anxiety (Fig. 1, symptom 3).

There was a statistically significant decrease in quantitative CBF in the hemispheres, brainstem, and cerebellum of approximately the same magnitude (6–8%), with no concomitant change in arterial $p\text{CO}_2$ (Tables 1 and 2).

SPM99 analysis identified statistically significant areas of relative CBF increase in bilateral thalamus, right globus pallidus, and bilateral MPFC (Table 3 and Fig. 2). Analysis of the Talairach

atlas coordinates places these activations in the dorsal medial thalamus, medial ventral globus pallidus, and areas 24 and 32 of the ACC. Because of the extent of the ventral pallidal activation, involvement of the nucleus accumbens cannot be excluded. Activations were seen also in the right sensorimotor cortex, right orbital prefrontal cortex (lateral portion of area 11), and right temporal cortex. Although increased flow was statistically significant only for the right hemisphere areas in the orbital prefrontal cortex, globus pallidus, and sensorimotor cortex, nonsignificant increases were observed in the left hemisphere as well. Careful visual examination of the normalized difference image revealed a small intense area of activation in the periaqueductal gray matter, which did not meet criteria for statistical significance because of the small number of voxels involved (Table 3 and Fig. 2). Computer simulation demonstrated that an actual increase in CBF of 60% in this small structure is necessary to produce the observed increase in the PET image because of the effects of partial volume averaging. There was no suggestion of activation in hypothalamus.

Significant relative reductions in CBF were observed in right hippocampus and right temporal cortex (Table 3 and Fig. 3). A symmetrical decrease was apparent in the left hippocampus that did not reach statistical significance. The magnitude of CBF reduction in bilateral hippocampus of $-26 \pm 12\%$ was substantially greater than that in the remainder of the brain.

Discussion

Overall Decreases in CBF. We observed a statistically significant decrease of 6–8% in quantitative CBF in the hemispheres, cerebellum, and brainstem, with a reduction in arterial plasma glucose to 3.0 mmol/liter. Previous studies of normal humans during hypoglycemia, including our own, reported no change in CBF with plasma glucose values down to 2.3 mmol/liter, with increases of 10–20% in CBF occurring at lower levels of 1.1–2.2 mmol/liter (32–39). As opposed to these other studies that used only one CBF measurement at each plasma glucose level, we performed four measurements at each level and averaged the

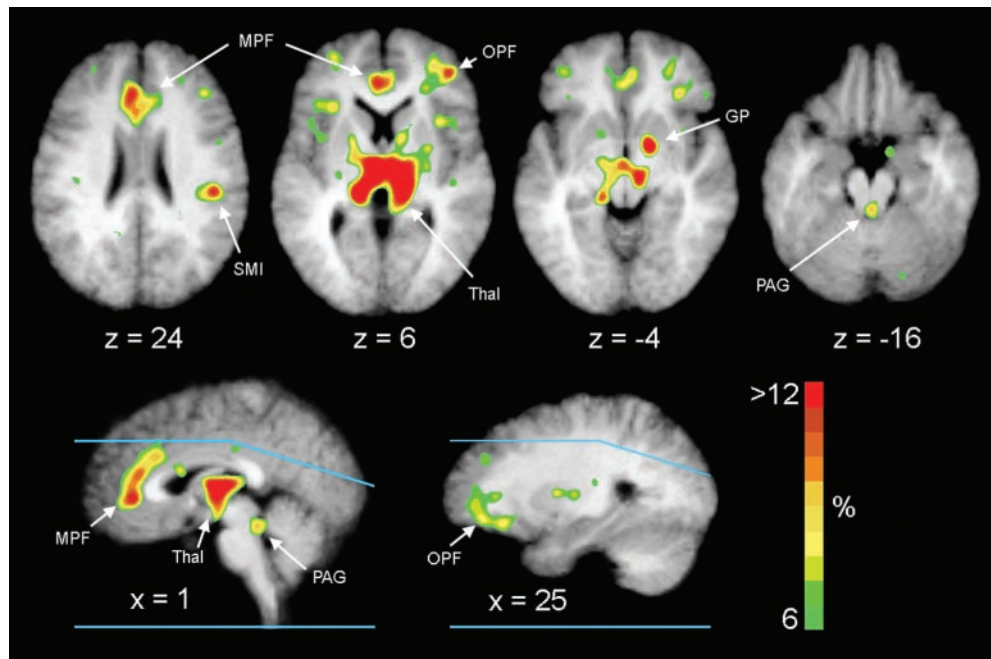


Fig. 2. Mean difference images of relative rCBF increases from nine subjects superimposed on the composite structural MR image. The color bar indicates percent increase relative to whole-brain flow and has been fixed at a maximum of 12%. Right brain is on the right. Blue lines on the sagittal sections show the upper and lower limits of brain sampled in all nine subjects. Flow is elevated in thalamus (Thal), MPFC (MPF), right orbital prefrontal cortex (OPF), right globus pallidus (GP), right sensorimotor cortex (SMI), and periaqueductal gray (PAG).

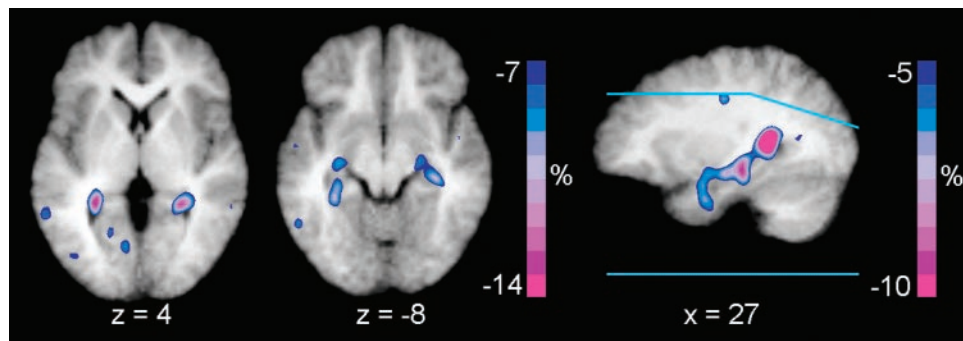


Fig. 3. Mean difference images of relative rCBF decreases from nine subjects superimposed on the composite structural MR image. The color bar indicates percent decrease relative to whole-brain flow and has been fixed at a minimum of -12% . Right brain is on the right. Blue lines on the sagittal section show the upper and lower limits of brain sampled in all nine subjects. Flow is decreased bilaterally in the hippocampus.

results. The reduction in CBF of 6–8% that we measured is similar to our test-retest variability for two consecutive quantitative CBF measurements of 7.7%. It is most likely that the improvement in precision that we gained by averaging four measurements permitted us to detect this small decrease. The physiological interpretation of this reduction in CBF is more speculative. The cerebral metabolic rate of glucose is decreased at plasma glucose levels of 3.0 mmol/liter (37, 40). The observed reduction in CBF in this study may be secondary to the reduction in metabolism, similar to that seen during barbiturate anesthesia (41).

Regional Changes in CBF. We used the indirect technique of measuring changes in rCBF to identify regions of increased neuronal activity during hypoglycemia. This approach requires that the physiological coupling between increases in neuronal activity and increases in rCBF remains intact under these conditions. We have shown previously that there is no change in the rCBF response to somatosensory stimulation with arterial hypoglycemia to 2.3 mmol/liter (42). Areas of increased CBF primarily reflect the increased metabolic activity of synaptic fields, not the spike firing rate of neuronal cell bodies (43, 44). The ability to detect areas of increased neuronal activity by changes in rCBF will depend on the spatial extent, magnitude, and consistency of the rCBF increase.

The MPFC is reciprocally connected to the dorsal medial thalamus and also projects to the nucleus accumbens and then to the ventral globus pallidus. This medial network also provides the major cortical output to autonomic structures in the hypothalamus and periaqueductal gray. The major structures that were activated during hypoglycemia (areas 24 and 32 of the ACC, medial ventral globus pallidus, and dorsal medial thalamus) are components of this medial output network (10). The orbital prefrontal cortex (lateral portion of area 11) is a component of the orbital prefrontal network that receives and integrates sensory information and interacts with the medial network (45). We also found evidence for activation of periaqueductal gray matter (which did not meet prespecified criteria for statistical significance) but not for the hypothalamus, although there was clear biochemical evidence of activation of the hypothalamic-pituitary axis (Table 1). Given the small size of these two structures, a very large increase in CBF would be necessary to detect a statistically significant change on the PET scans with the criteria that we set. Thus, the absence of a detectable CBF change in hypothalamus should not be interpreted as evidence against activation of hypothalamic neurons during hypoglycemia.

Our data demonstrate activation by hypoglycemia of a distributed network including the ACC, basal ganglia, and autonomic brainstem structures that corresponds closely to the

neuroanatomical description of the major efferent system arising from the MPFC (10, 45). Because increased rCBF indicates increased synaptic activity in the region, the activation observed in the anterior cingulate region is interpreted best as increased activity from afferent projections or interneurons. Increased output from activity of neuronal cell bodies in the ACC output is reflected as increased CBF in projections to thalamus, globus pallidus, and periaqueductal gray. Although it is not possible to determine from this experiment where afferent projections to ACC arises, our results suggest that the ACC may serve as an area in which visceral sensory inputs are linked to autonomic output.

We also identified increased flow in the sensorimotor cortical representation of the jaw. This is consistent with teeth clenching that appeared as increased blood flow in the jaw muscles of 6 of the subjects. There was a decrease in rCBF to hippocampus bilaterally that was statistically significant in the right hemisphere. The hippocampus is particularly sensitive to damage from more severe levels of hypoglycemia (46, 47). The selectively greater reduction in hippocampal CBF that we observed may indicate more severe impairment in glucose metabolism at these more moderate levels of hypoglycemia in these structures as compared with the remainder of the brain.

A previous study of rCBF in diabetic subjects during normoglycemia and hypoglycemia showed increased CBF in bilateral superior frontal cortex and right thalamus with decreases in the right posterior cingulate and right putamen (48). Because all subjects were people with diabetes mellitus who had suffered repeat episodes of hypoglycemia from insulin treatment, it is difficult to interpret these findings in contrast to our own.

Connections between the MPFC and autonomic nervous system have been recognized for >100 years (9). In humans, the role of the MPFC in the modulation of autonomic states has been addressed primarily in studies of complex, “high-level” behaviors involving effortful cognitive and volitional motor tasks, emotion, and social judgements (5, 12, 15, 49). No role of cortical structures in modulating “low-level” autonomic responses to basic physiological states in humans has been demonstrated. Such responses are generally considered to involve subcortical structures only (12, 15). In this study, we demonstrated activation of the ACC as part of a distributed system involving the autonomic response to hypoglycemia. This basic physiological response was associated with little evidence of cognitive or emotional stress, indicating the primary participation of the frontal cortex in modulation of autonomic responses to basic physiological stimuli.

We thank Krishan Jethi, Cornell Blake, Joy Brothers, Zina Lubovich, Michael Morris, Lori-McGee-Minnich, Lennis Lich, Susanne Fritsch,

John Hood, and the Washington University Medical School cyclotron staff for technical assistance. Steven Petersen, Joel Price, and

Marcus Raichle provided helpful comments. This work was supported by U.S. Public Health Service Grants DK27085, RR00036, and NS41771.

1. Bush, G., Luu, P. & Posner, M. I. (2000) *Trends Cogn. Sci.* **4**, 215–222.
2. Phan, K. L., Wager, T., Taylor, S. F. & Liberzon, I. (2002) *Neuroimage* **16**, 331–348.
3. Bechara, A., Damasio, H., Tranel, D. & Damasio, A. R. (1997) *Science* **275**, 1293–1295.
4. Critchley, H. D., Mathias, C. J. & Dolan, R. J. (2001) *Neuron* **29**, 537–545.
5. Critchley, H. D., Elliott, R., Mathias, C. J. & Dolan, R. J. (2000) *J. Neurosci.* **20**, 3033–3040.
6. Devinsky, O., Morrell, M. J. & Vogt, B. A. (1995) *Brain* **118**, 279–306.
7. Wood, J. N. & Grafman, J. (2003) *Nat. Rev. Neurosci.* **4**, 139–147.
8. Simpson, J. R., Jr., Drevets, W. C., Snyder, A. Z., Gusnard, D. A. & Raichle, M. E. (2001) *Proc. Natl. Acad. Sci. USA* **98**, 688–693.
9. Neafsy, E. J. (1990) in *Progress in Brain Research*, eds Uylings, H. B. M., Van Eden, C. G., DeBruin, J. P. C., Corner, M. A. & Feenstra, M. G. P. (Elsevier, New York), pp. 147–166.
10. Ongur, D. & Price, J. L. (2000) *Cereb. Cortex* **10**, 206–219.
11. Critchley, H. D., Corfield, D. R., Chandler, M. P., Mathias, C. J. & Dolan, R. J. (2000) *J. Physiol. (London)* **523**, 259–270.
12. Damasio, A. R., Tranel, D. & Damasio, H. (1990) *Behav. Brain Res.* **41**, 81–94.
13. Borg, M. A., Sherwin, R. S., Borg, W. P., Tamborlane, W. V. & Shulman, G. I. (1997) *J. Clin. Invest.* **99**, 361–365.
14. Cranston, I., Reed, L. J., Marsden, P. K. & Amiel, S. A. (2001) *Diabetes* **50**, 2329–2336.
15. Critchley, H. D., Mathias, C. J., Josephs, O., O'Doherty, J., Zanini, S., Dewar, B. K., Cipolotti, L., Shallice, T. & Dolan, R. J. (2003) *Brain* **126**, 2139–2152.
16. Towler, D. A., Havlin, C. E., Craft, S. & Cryer, P. (1993) *Diabetes* **42**, 1791–1798.
17. Shah, S. D., Clutter, W. E. & Cryer, P. E. (1985) *J. Lab. Clin. Med.* **106**, 624–629.
18. Kuzuya, H., Blix, P. M., Horwitz, D. L., Steiner, D. F. & Rubenstein, A. H. (1977) *Diabetes* **26**, 22–29.
19. Ensink, J. (1983) in *Handbook of Experimental Pharmacology*, ed. Lefebvre, P. (Springer, New York), pp. 203–221.
20. Gingerich, R. L., Lacy, P. E., Chance, R. E. & Johnson, M. G. (1978) *Diabetes* **27**, 96–101.
21. Farmer, R. W. & Pierce, C. E. (1974) *Clin. Chem. (Washington, D.C.)* **20**, 411–414.
22. Schalch, D. & Parker, M. (1964) *Nature* **703**, 1141–1142.
23. Wienhard, K., Dahlbom, M., Eriksson, L., Michel, C., Bruckbauer, T., Pietrzyk, U. & Heiss, W.-D. (1994) *J. Comput. Assist. Tomogr.* **18**, 110–118.
24. Herscovitch, P., Markham, J. & Raichle, M. E. (1983) *J. Nucl. Med.* **24**, 782–789.
25. Raichle, M. E., Martin, W. R. W., Herscovitch, P., Mintun, M. A. & Markham, J. (1983) *J. Nucl. Med.* **24**, 790–798.
26. Videen, T. O., Perlmutter, J. S., Herscovitch, P. & Raichle, M. E. (1987) *J. Cereb. Blood Flow Metab.* **7**, 513–516.
27. Woods, R. P., Mazziotta, J. C. & Cherry, S. R. (1993) *J. Comput. Assist. Tomogr.* **17**, 536–546.
28. Woods, R. P., Cherry, S. R. & Mazziotta, J. C. (1992) *J. Comput. Assist. Tomogr.* **16**, 620–633.
29. Talairach, J. & Tournoux, P. (1988) *Co-Planar Stereotaxic Atlas of the Human Brain* (Thieme, New York).
30. Friston, K. J., Holmes, A. P., Worsley, K. J., Poline, J. P., Frith, C. D. & Frackowiak, R. S. J. (1995) *Hum. Brain Mapp.* **2**, 189–210.
31. Worsley, K. J., Marrett, S., Neelin, P., Vandal, A. C., Friston, K. J. & Evans, A. C. (1996) *Hum. Brain Mapp.* **4**, 58–73.
32. Gottstein, U. & Held, K. (1967) *Klin. Wochenschr.* **45**, 18–23.
33. Eisenberg, S. & Seltzer, H. S. (1962) *Metabolism* **11**, 1162–1168.
34. Neil, H. A., Gale, E. A., Hamilton, S. J., Lopez-Espinoza, I., Kaura, R. & McCarthy, S. T. (1987) *Diabetologia* **30**, 305–309.
35. Tallroth, G., Ryding, E. & Agardh, C.-D. (1992) *Metabolism* **41**, 717–721.
36. Powers, W. J., Boyle, P. J., Hirsch, I. B. & Cryer, P. E. (1993) *Am. J. Physiol.* **265**, R883–R887.
37. Boyle, P. J., Nagy, R. J., O'Conner, A. M., Kempers, S. F., Yeo, R. A. & Qualls, C. (1994) *Proc. Natl. Acad. Sci. USA* **91**, 9352–9356.
38. Boyle, P. J., Kempers, S. F., O'Conner, A. M. & Nagy, R. J. (1995) *N. Engl. J. Med.* **333**, 1726–1731.
39. Eckert, B., Ryding, E. & Agardh, C. D. (1998) *Diabetes Res. Clin. Pract.* **40**, 91–100.
40. Madsen, P. L., Holm, S., Herning, M. & Lassen, N. A. (1993) *J. Cereb. Blood Flow Metab.* **13**, 646–655.
41. Astrup, J., Sorensen, P. M. & Sorensen, H. R. (1981) *Stroke (Dallas)* **12**, 726–730.
42. Powers, W. J., Hirsch, I. B. & Cryer, P. (1996) *Am. J. Physiol.* **270**, H554–H559.
43. Schwartz, W. J., Smith, C. B., Davidsen, L., Savaki, H., Sokoloff, L., Mata, M., Fink, D. J. & Gainer, H. (1979) *Science* **205**, 723–725.
44. Mathiesen, C., Caesar, K., Akgoren, N. & Lauritzen, M. (1998) *J. Physiol. (London)* **512**, 555–566.
45. Ongur, D., Ferry, A. T. & Price, J. L. (2003) *J. Comp. Neurol.* **460**, 425–449.
46. Auer, R. N. & Siesjo, B. K. (1988) *Ann. Neurol.* **24**, 699–707.
47. Fujioka, M., Okuchi, K., Hiramoto, K. I., Sakaki, T., Sakaguchi, S. & Ishii, Y. (1997) *Stroke (Dallas)* **28**, 584–587.
48. MacLeod, K. M., Gold, A. E., Ebmeier, K. P., Hepburn, D. A., Deary, I. J., Goodwin, G. M. & Frier, B. M. (1996) *Metabolism* **45**, 974–980.
49. Koski, L. & Paus, T. (2000) *Exp. Brain Res.* **133**, 55–65.